Supporting Information

Interpenetrated biosurfactant-silk fibroin networks - A SANS study

Andrea Lassenberger,*,[1] Anne Martel,[1] Lionel Porcar,[1] Niki Baccile*,[2]

[1]Institut Laue-Langevin, 71 Avenue des Martyrs, 38042 Grenoble Cedex 9, France
[2]Centre National de la Recherche Scientifique, Laboratoire de Chimie de la Matière Condensée de Paris, LCMCP, Sorbonne Université, Paris F-75005, France

Contents

1. SDS-PAGE of regenerated silk fibroin (SF)

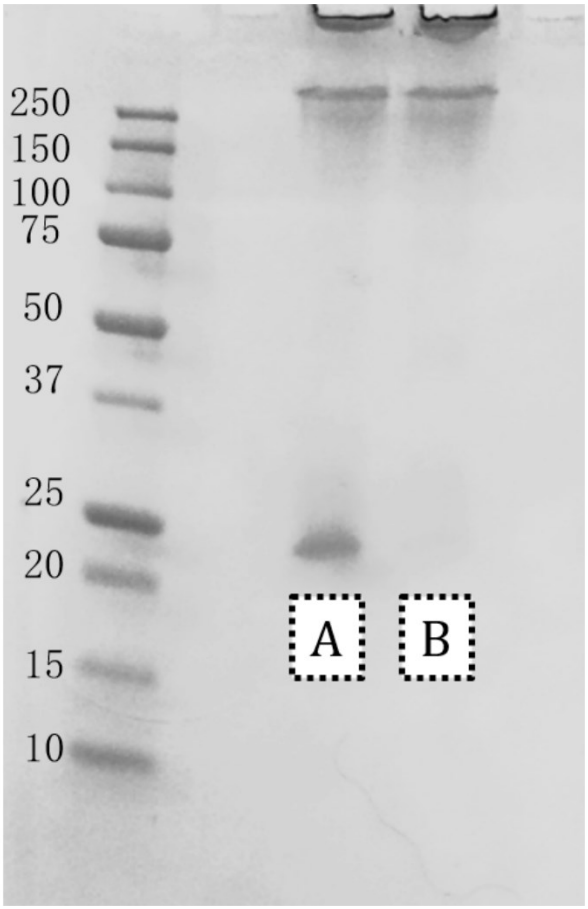

Figure S 1. SDS-PAGE of SF solution after dialysis in H_2O. Band **A)** The disulfide bond between the light chain (FibL) and the heavy chain (FibH) was cleaved with β-mercaptoethanol, resulting in two distinct bands at >250 kDa (FibH) and ~25 kDa (FibL). Band **B)** SF without treatment of β-mercaptoethanol resulting in a single band >250 kDa.

2. SANS fitting approach

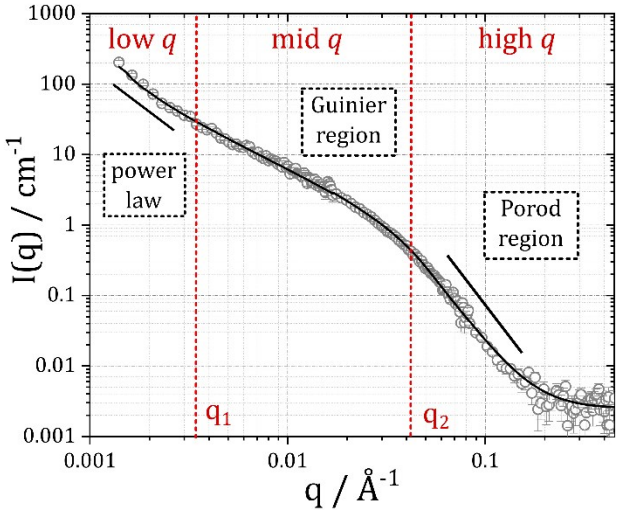

Figure S 2 Representative SF neutron scattering pattern with q-regions discussed in the main manuscript. The characteristic length scales q_1 and q_2, described in equation 2 in the main text are illustrated in red with $q_1 \approx 0.0035$ Å^{-1} and $q_2 \approx 0.04$ Å^{-1}.

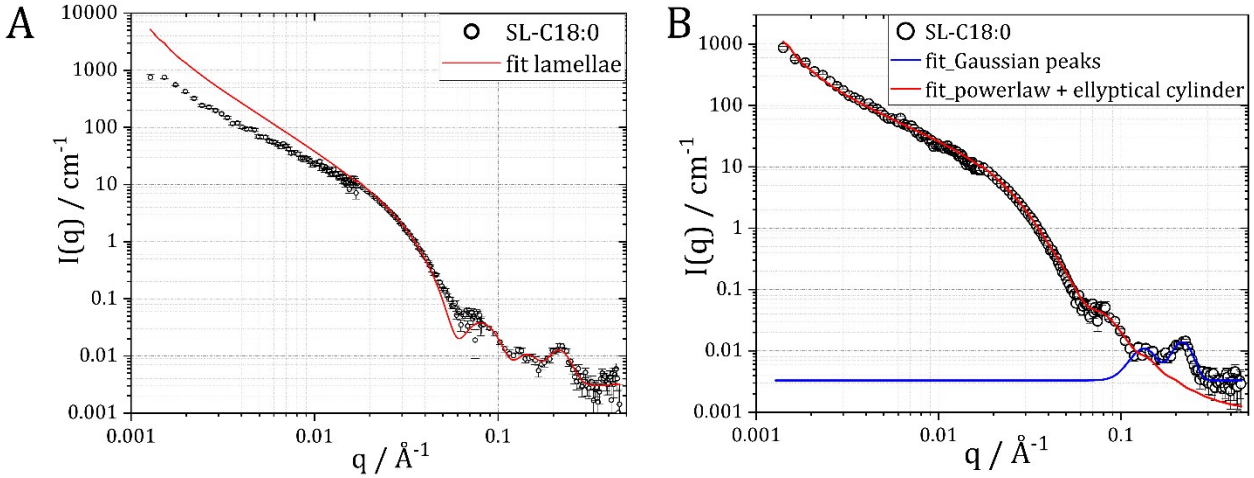

Figure S 3. SANS fitting approaches for SL-C18:0. **A)** Approach with a model for a lamellar phase. **B)** Model combination of a power law + elliptical cylinder (red) and two Gaussian peaks (blue). It is noteworthy the first Gauss peak coincides with the second oscillation of the elliptical cylinder form factor whereas the third peak known to be the repeating inter-lipid distance in the twisted ribbons formed by SL-C18:0 [1]. Open symbols represent the experimental data, continuous lines the fits.

3. Calculation of neutron scattering length densities.

The SLD of sophorolipids was calculated with SasView as $SLD\ (SL)_{head}$ being the SLD of the hydrophilic sugar headgroups and $SLD\ (SL)_{tail}$ as the SLD of the hydrophobic saturated (SL-C18:0) or mono-unsaturated (SL-C18:1) oleic or stearic acid derived tail. H-D exchange was taken into account. The different head and tail $SLDs$ were only taken into account for SL-C18:1. For the fitting of SL-C18:0 we considered only $SLD\ (SL)_{tail}$ for simplicity. The SLD of SF was calculated with the biomolecular SLD

calculator available on the ISIS homepage[2] by using the amino acid sequence provided from UniProt[3] and an estimated H-D exchange of 90 %:

SL-C18:1 (in D_2O): $SLD\ (SL)_{head} = 2.88 \cdot 10^{-6}Å^{-2}$, $SLD\ (SL)_{tail} = 0.25 \cdot 10^{-6}Å^{-2}$,

SL-C18:0 (in 100 % D_2O): $SLD\ (SL)_{tail} = 0.19 \cdot 10^{-6}Å^{-2}$, in 51 % D_2O: $SLD\ (SL)_{tail} = 0.1 \cdot 10^{-6}Å^{-2}$

$SLD\ (SF)_{D2O} = 3.66 \cdot 10^{-6}Å^{-2}$, $SLD\ (SF)_{H2O} = 2.3 \cdot 10^{-6}Å^{-2}$,

$SLD_{D2O} = 6.3 \cdot 10^{-6}Å^{-2}$, $SLD_{H2O} = -0.56 \cdot 10^{-6}Å^{-2}$

4. SANS models

Samples were fitted with the following model combinations:
SL-C18:1 – core-shell ellipsoid[4]
SL-C18:0 – power law + elliptical cylinder[5] + 2 Gaussian peaks
SF gelled (D_2O) – power law + Guinier-Porod
SF-SL-C18:1 - power law + Guinier-Porod + core-shell ellipsoid
SF-SL-C18:0 - power law + Guinier-Porod + power law + elliptical cylinder + 2 Gaussian peaks

The volume fractions Φ ('scale') were held constant throughout the whole fitting process

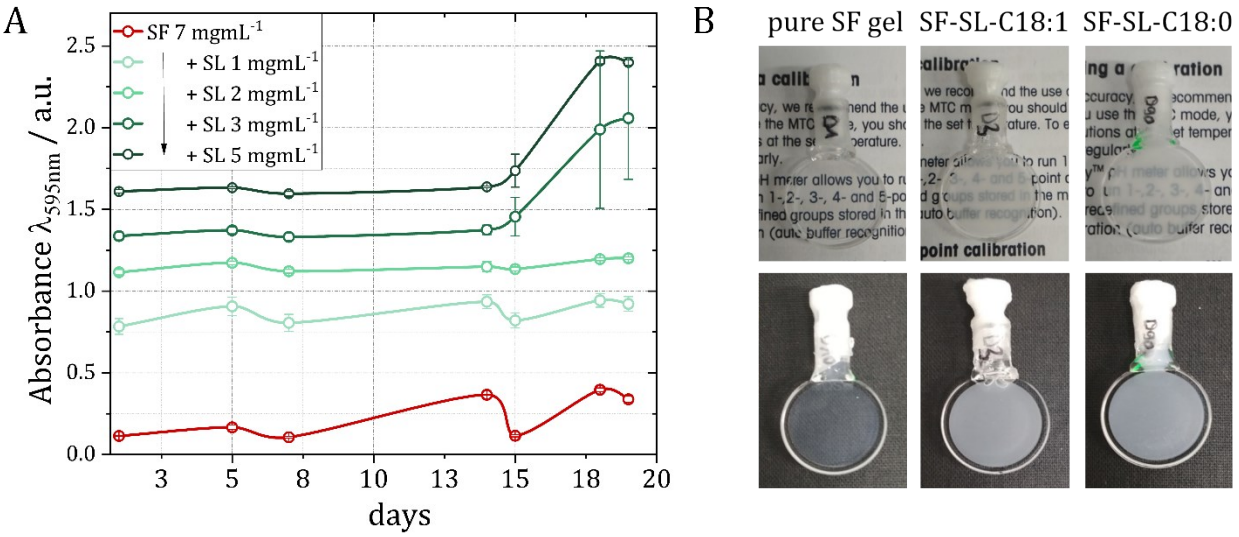

Figure S 4. A) Absorption measurements at 595 nm for SF at 7 mgmL-1 and SF-SL-C18:0 composite gels at the indicated lipid concentrations. Results are presented for completeness but not used for interpretation. **B)** Photographs of SF gels and composite gels in D_2O in the SANS measurement cells, showing that all gels are homogenous.

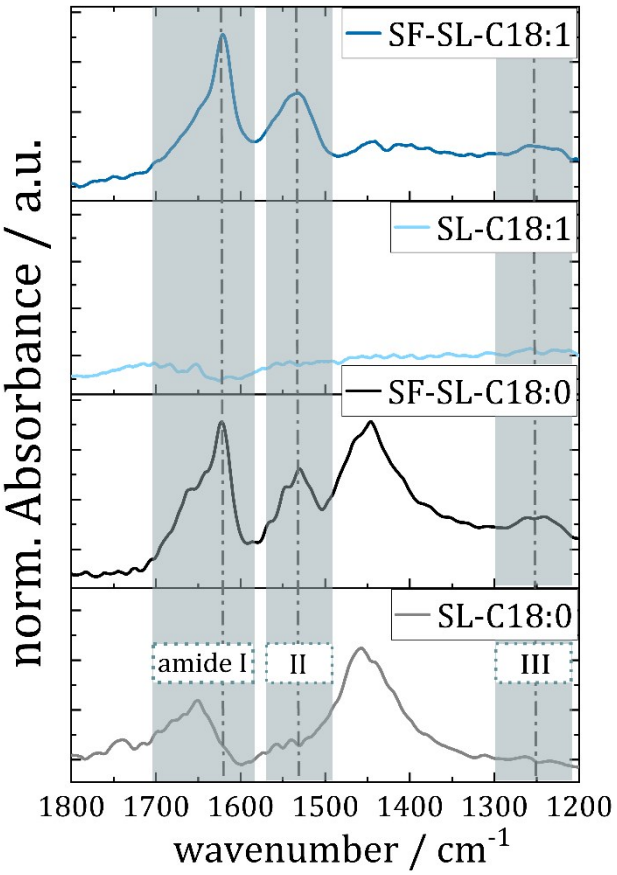

Figure S 5. ATR-FTIR spectra of composite gels and the respective lipids in H_2O from top to bottom: SF-SL-C18:1 composite, SL-C18:1 at 5 mgmL^{-1}, SF-SL-C18:0 composite and SL-C18:0 lipid at 5 mgmL^{-1}. Spectra were normalized to the maximum absorption in the amide I band at 1696 cm^{-1}. The amide I, II and III regions are highlighted to show that there is no interference of the lipid bands with the peaks discussed in the main manuscript for determination of secondary structure. Note that at such small concentrations and measurement in H_2O the COOH band of SL at 1704 cm^{-1} is absent. The broad peak between 1400 and 1500 cm^{-1} in the SL-C18:0 spectrum can be assigned to scissoring (δ) of CH_2 and stretching (ν) of CO and CC groups in the carbohydrate part of SL and the ν_s of COO^-. The peak is absent in SL-C18:1 since an ATR geometry was used. SL-C18:0 is a gel with solid assemblies that adsorbs to the crystal, resulting in much higher absorption than SL-C18:0, which is liquid.

5. Inverse approach: subtracting SF from the composite signal (SANS)

To further support our hypothesis that the structure of the employed lipids is intact, in particular that of SL-C18:1 for which contrast matching experiments were less striking than for SL-C18:0, we subtracted the scattering intensity of pure SF from that of the composite gels and compared it with that of the pure lipids. Figure S6A displays the resulting curve $I(q)_{SF-SL-C18:1} - I(q)_{SF}$ (grey) and Figure 6B shows $I(q)_{SF-SL-C18:0} - I(q)_{SF}$, plotted together with the respective pure lipid. In Figure S6A (grey) the signal of the pure lipid is recovered at $q > 0.025$ Å and fitted with the same core-shell ellipsoid model as pure SL-C18:1, letting the values for core, shell and axis ratio and background vary. The fitted parameters (Table S1) are very close to that of the pure lipid, supporting our hypothesis that the structure of SL-C18:1 micelles does not change in presence of SF. The difference in scattering intensity at $q < 0.025$ Å stems from the change in shape of SF and the increased network inhomogeneities as is described in the main manuscript. One could argue that the change in signal intensity at low q stems from a change in shape of SL-C18:1. This however could be ruled out with contrast matching experiments (see section 5) where SF is matched with the resulting signal being flat at low q.

In Figure S6B the signal $I(q)_{SF-SL-C18:0} - I(q)_{SF}$ is fitted with the same combined power law – elliptical cylinder – gauss peak model as pure SL-C18:0 by varying the values for cylinder diameter, axis ratio and background (Table S1). The resulting difference is much less pronounced and the signal of the pure lipid is almost completely recovered, which is in line with contrast matching experiments for this system.

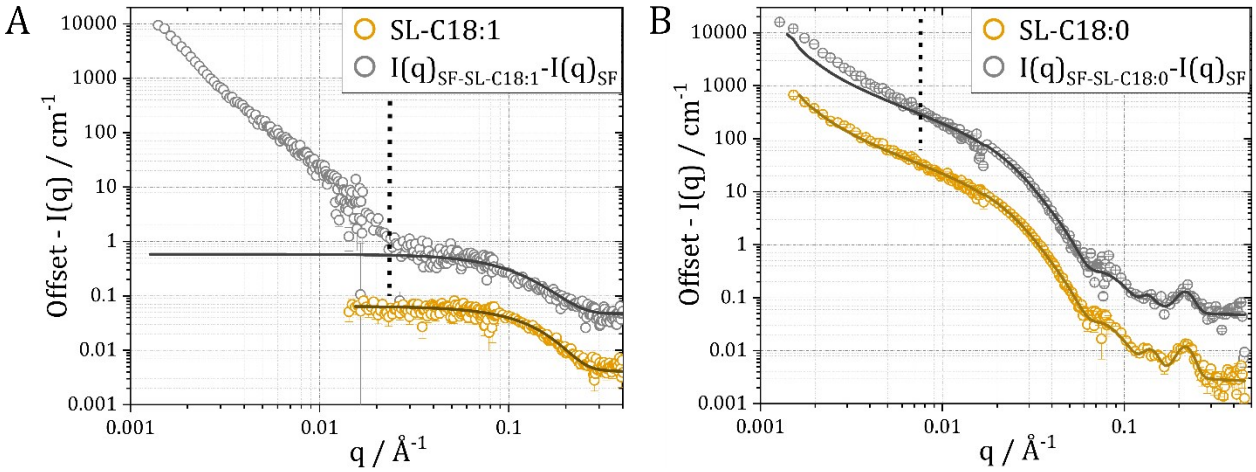

Figure S 6. Neutron scattering data of hydrogels four weeks after dialysis and lipids, all in D_2O with SF at 7 mgmL^{-1} and SL at 5 mgmL^{-1}. The signal of SF gelled is subtracted from the signal of the composite gels yielding the curves **A)** $I(q)_{SF-SL-C18:1} - I(q)_{SF}$ (grey), plotted together with $I(q)$ of pure SL-C18:1 and **B)** $I(q)_{SF-SL-C18:0} - I(q)_{SF}$ (grey), displayed with the signal for pure SL-C18:0. The grey curves are fitted with the same models and similar parameters (cf. Table S1) as the pure lipids. The vertical lines mark where the model deviates significantly from the data. Above this q value the signal of the respective lipid is fully recovered whereas below it, the resulting signal intensity stems from changes in the overall network structure.

6. Contrast matching experiments

SF-SL-C18:1 was attempted to be measured under contrast matching conditions (Figure S7). We aimed to measure at 51 % D_2O, which is the match point of SF, to gain information about the integrity of SL-C18:1 micelles. However, the scattering intensity of SL-C18:1 is already quite low in D_2O at the chosen concentration and the signal was lost almost completely in the incoherent background at 51 % D_2O, also for the pure lipid (Figure S7, yellow). The only information that we can extract from this is, that the SL-C18:1 micelles did not form e.g. worm-like micelles or other aggregates in presence of SF as this would result in an increase of scattering intensity at low q, visible at contrast matching conditions.[6]

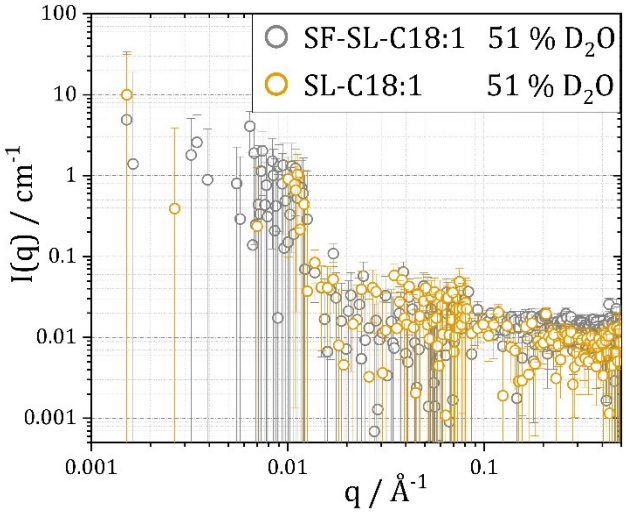

Figure S 7. SANS data for SF-SL-C18:1 composite gel (grey) and pure SL-C18:1 (yellow) at the match point of SF (51 % D_2O). The signal of SL is lost in high incoherent scattering background stemming from 49 % H_2O. At low q only very diffuse scattering intensity is observed, supporting the hypothesis that the scattering difference observed in Figure S6A stems only from a change in network structure. If SL-C18:1 would have formed e.g. wormlike micelles, it would be visible under contrast matching conditions in an increase of $I(q)$ at low q.

In addition to the discussed contrast matching experiments, we have considered to perform measurements at the match point of the sophorolipids. This is however not straight forward since the head- and tail of SL have two very different

match points, whereas the match point for the sophorose headgroup is very close to that of SF (49 % D_2O vs. 51 % D_2O for SF). The match point of the aliphatic tail is at 8 % D_2O, which causes a high incoherent background. We opted thus for matching SF.

Table S 1. Fitted parameters for sophorolipids in pure micellar (SL-C18:1) and ribbon containing form (SL-C18:0) and in the composite hydrogels. Values for lipids in the composite gels were obtained by feeding the fitted parameters for SF (*cf.* Table 1 in the main text) into the model for the composite and then allowing the parameters for radius and axis ratio for SL to vary. Alternatively, the signal of SF was subtracted from that of the composite and the resulting signal was fitted with a core-shell ellipsoid model (SL-C18:1) or a combination of power law-elliptical cylinder-gauss peak (SL-C18:0).

	$solvent$ /%D	SLD / $x10^{-6}$Å^{-2}		$radius_{min}$ / Å	$radius_{maj}$ /Å	t_{shell} /Å	$peakpos$ /Å^{-1}
		tail	**head**				
SL-C18:1	100	0.3	2.88	5 ± 0.1	20 ± 0.3	9 ± 0.9	-
SL-C18:1 in comp gel ($I(q)_{SF\text{-}SL\text{-}C18:1}$-$I(q)_{SL\text{-}C18:1}$)	100	0.3	2.88	5 ± 0.3	24 ± 0.4	7 ± 1.0	-
SL-C18:1 in comp gel ($I(q)_{SF\text{-}SL\text{-}C18:1}$-$I(q)_{SF}$)	100	0.3	2.88	5 ± 0.3	23 ± 0.5	8 ± 0.2	-
SL-C18:0	100	0.19	-	53 ± 0.2	122 ± 0.5	-	0.217
SL-C18:0 in comp gel ($I(q)_{SF\text{-}SL\text{-}C18:0}$-$I(q)_{SL\text{-}C18:0}$)	100	0.19	-	49 ± 0.1	122 ± 0.5	-	0.217
SL-C18:0 in comp gel ($I(q)_{SF\text{-}SL\text{-}C18:0}$-$I(q)_{SF}$)	100			55 ± 0.2	122 ± 0.4	-	0.217
SL-C18:0	51	0.1	-	53 ± 0.3	116 ± 0.5	-	-
SL-C18:0 in comp. gel	51	0.1	-	55 ± 0.2	119 ± 0.6	-	-

7. References

1. A.-S.Cuvier, J. Berton, C. V. Stevens, G. C. Fadda, F. Babonneau, I. N. A. Van Bogaert, W. Soetaert, G. Pehau-Arnaudet and N. Baccile, *Soft Matter,* **2014,** 10, 3950-3959.
2. http://psldc.isis.rl.ac.uk/Psldc/.
3. https://www.uniprot.org.
4. M. Kotlarchyk and S. H. Chen, *J. Chem. Phys.,* **1983,** 79, 2461-2469.
5. L. A. Feigin, and D. I. Svergun, *Structure analysis by small-angle X-ray and neutron scattering.* Plenum Press, New York, 1989.
6. P. Malo de Molina and M. Gradzielski, *Gels,* **2017,** 3 , 1-30.